

## Article

# Identification of YWHAH as a Novel Brain-Derived Extracellular Vesicle Marker Post Long-Term Midazolam Exposure during Early Development

Nghi M. Nguyen <sup>1,2,†</sup>, Daniel Meyer <sup>1,†</sup>, Luke Meyer <sup>1</sup>, Subhash Chand <sup>1</sup>, Sankarasubramanian Jagadesan <sup>2</sup>, Maireen Miravite <sup>1</sup>, Chittibabu Guda <sup>2</sup>, Sowmya V. Yelamanchili <sup>1,2</sup> and Gurudutt Pendyala <sup>1,2,3,4,\*</sup>

<sup>1</sup> Department of Anesthesiology, University of Nebraska Medical Center (UNMC), Omaha, NE 68198, USA

<sup>2</sup> Department of Genetics, Cell Biology, and Anatomy, University of Nebraska Medical Center (UNMC), Omaha, NE 68198, USA

<sup>3</sup> Child Health Research Institute, University of Nebraska Medical Center (UNMC), Omaha, NE 68198, USA

<sup>4</sup> National Strategic Research Institute, University of Nebraska Medical Center (UNMC), Omaha, NE 68198, USA

\* Correspondence: gpendyala@unmc.edu; Tel.: +1-402-559-8690

† These authors contributed equally to this work.

**Abstract:** Recently, the long-term use of sedative agents in the neonatal intensive care unit (NICU) has raised concerns about neurodevelopmental outcomes in exposed neonates. Midazolam (MDZ), a common neonatal sedative in the NICU, has been suggested to increase learning disturbances and cognitive impairment in children. However, molecular mechanisms contributing to such outcomes with long-term MDZ use during the early stages of life remain unclear. In this study, we for the first time elucidate the role of brain-derived extracellular vesicles (BDEVs), including mining the BDEV proteome post long-term MDZ exposure during early development. Employing our previously established rodent model system that mimics the exposure of MDZ in the NICU using an increasing dosage regimen, we isolated BDEVs from postnatal 21-days-old control and MDZ groups using a differential sucrose density gradient. BDEVs from the control and MDZ groups were then characterized using a ZetaView nanoparticle tracking analyzer and transmission electron microscopy analysis. Next, using RT-qPCR, we examined the expression of key ESCRT-related genes involved in EV biogenesis. Lastly, using quantitative mass spectrometry-based proteomics, we mined the BDEV protein cargo that revealed key differentially expressed proteins and associated molecular pathways to be altered post long-term MDZ exposure. Our study characterized the proteome in BDEV cargo from long-term MDZ exposure at early development. Importantly, we identified and validated the expression of YWHAH as a potential target for further characterization of its downstream mechanism and a potential biomarker for the early onset of neurodevelopment and neurodegenerative diseases. Overall, the present study demonstrated long-term exposure to MDZ at early development stages could influence BDEV protein cargo, which potentially impact neural functions and behavior at later stages of development.

**Keywords:** 14-3-3 eta; Midazolam; NICU; extracellular vesicles; proteomics; neurodevelopment



**Citation:** Nguyen, N.M.; Meyer, D.; Meyer, L.; Chand, S.; Jagadesan, S.; Miravite, M.; Guda, C.; Yelamanchili, S.V.; Pendyala, G. Identification of YWHAH as a Novel Brain-Derived Extracellular Vesicle Marker Post Long-Term Midazolam Exposure during Early Development. *Cells* **2023**, *12*, 966. <https://doi.org/10.3390/cells12060966>

Academic Editors: Fabiana Geraci, Maria Magdalena Barreca and Carl D. Richards

Received: 6 January 2023

Revised: 10 February 2023

Accepted: 15 March 2023

Published: 22 March 2023



**Copyright:** © 2023 by the authors. Licensee MDPI, Basel, Switzerland. This article is an open access article distributed under the terms and conditions of the Creative Commons Attribution (CC BY) license (<https://creativecommons.org/licenses/by/4.0/>).

## 1. Introduction

In the Neonatal Intensive Care Unit (NICU), it is common for neonates to undergo frequent and strenuous life-saving procedures [1]. While the limitation of these procedures is ideal for avoiding the use of analgesics and sedatives, this is not always possible. Early-stage neurodevelopment is a delicate and precise process, and as potent modifiers of signaling pathways essential to neurodevelopment, the use of these substances may potentially have adverse effects on the future neural health of NICU patients [2]. Therefore, the careful exploration of the long-term effects of these drugs is essential to determine

which are safe for continued use. One of these commonly used sedatives is Midazolam (MDZ), a benzodiazepine frequently used to manage seizures and alleviate stress prior to surgery [3,4]. In previous studies, exposure to Midazolam has been linked to apoptotic neurodegeneration in the cerebral cortex and caudate nucleus and decreased hippocampal volume [1,5]. Furthermore, our lab has previously identified alterations in the synaptic proteome associated with long-term MDZ exposure, suggesting potential disturbances in neural plasticity and cytoskeletal architecture [3]. However, a comprehensive understanding of MDZ-induced effects on cellular composition and function is yet to be established. One crucial target for future studies is the brain-derived extracellular vesicle (BDEV). BDEV refers to a diverse group of membrane-bound nanovesicles, generally organized by origin and size as either exosomes, microvesicles, or apoptotic bodies [6]. Briefly, exosomes are phospholipid-bilayer bound vesicles ranging in size from about 50–100 nm and generated by exocytosis of multivesicular bodies. Microvesicles range from about 100–1000 nm and form via budding from the plasma membrane. Apoptotic bodies are 1–5  $\mu\text{m}$  in diameter and are formed as blebs released from cells performing apoptosis [7]. BDEVs serve a wide variety of purposes, including conveying immune response [7,8], initiation of oncogenic cellular transformation [7,9], and lateral gene transfer [7,10], and contain diverse molecular cargo, including lipids, RNA, and protein [11]. As important facilitators of intercellular communication, cellular motility, cellular polarization, and even diseases including neurodegeneration and cancer, BDEVs represent a promising target for the study, as well as a therapeutic treatment, of MDZ-induced neural impairments [12,13]. For the first time, the current study utilized high-throughput mass spectrometry-based proteomics to identify differentially expressed proteins, as well as Gene Ontology (ClueGO) application to analyze our proteomic data and identify key differentially regulated molecular functions and biological processes associated with MDZ exposed BDEVs.

## 2. Materials and Methods

### 2.1. Animals

Pregnant Sprague–Dawley rats were obtained from Charles River Laboratories Inc. (Wilmington, MA, USA) and group-housed individually in a 12 h light-dark cycle. All animals were fed ad libitum and allowed to give birth naturally. All procedures and protocols were approved by the Institutional Animal Care and Use Committee (IACUC) of the University of Nebraska Medical Center (IACUC protocol: 19-130-01-EP) and conducted in accordance with the National Institutes of Health Guide for the Care and Use of Laboratory Animals.

### 2.2. Midazolam Treatment

The preclinical model system and the dosage regimen employed in this study have been established in our previously published work [3]. Briefly, at postnatal day (P) 3, rats were given subcutaneous injections of 1 mg/kg MDZ and ramped up to 10 mg/kg/day using the dose-escalation method until P21. Pups only received a single injection per day, following which they were placed beneath a heat lamp to maintain body temperature and were monitored for any distresses. Pups' reflexes including posture, tail, cornea, and righting reflex were indicated as proper sedation. Brains were extracted at P21 1 h after the last treatment and stored at  $-80\text{ }^{\circ}\text{C}$  for subsequent EV isolation.

### 2.3. BDEV Isolation

BDEVs were isolated using a sucrose density gradient as described in our previous studies [11,14,15]. Briefly, 450 mg of brain tissue was subjected to EV isolation. Brain tissue was homogenized and digested in 3.5 mL Hibernate A (HA) with 20 units/mL papain solution for 15 min at  $37\text{ }^{\circ}\text{C}$ . After 15 min of incubation in  $37\text{ }^{\circ}\text{C}$ , 6.5 mL HA containing antipain and protease inhibitor was added to the homogenized solution to stop the reaction. The solution was then centrifuged several times (at  $300\times g$  and  $2000\times g$  for 10 min, and  $10,000\times g$  for 30 min at  $4\text{ }^{\circ}\text{C}$ ) to eliminate cellular debris and residual cells. The supernatant

was then passed through a 0.22  $\mu\text{m}$  syringe filter (Corning Incorporated (catalog # 431219), Corning, distributed by Thermo Scientific, Waltham, MA, USA). To maximize EV yield, samples were ultracentrifuged at  $100,000\times g$  for an hour at  $4^\circ\text{C}$ , followed by purification using a density gradient separation technique. For the density gradient separation, sucrose concentrations ranging from 0.25 to 2 M were used, and the concentrated EVs pellet was resuspended in the 0.95 M layer and ultra-centrifuged at  $200,000\times g$  for 16 h at  $4^\circ\text{C}$ . To obtain the purified EV pellet, fractions enhanced with EVs were subjected to additional ultracentrifugation at  $100,000\times g$ . These EV pellets were then resuspended in particle-free phosphate-buffered saline (PBS), and their protein content was determined using a BCA Protein Assay Kit (Thermo Scientific, Waltham, MA, USA) per the manufacturer's manual.

#### 2.4. BDEV Markers Validation

To establish the purity of the BDEVs, we examined the expression of positive markers: Hsp70 (SAB4200714, Sigma-Aldrich, St. Louis, MO, USA), Flot-1 (abcam41927, Abcam, Cambridge, UK), CD81 (MCA1846, Bio-Rad Laboratories, Inc., Hercules, CA, USA), CD63 (BD551458, BD Biosciences, Franklin Lakes, NJ, USA), HSP90 (C45G5, Cell Signaling Technology, DANVERS, MA, USA), and negative marker GM130 (BD610822, BD Biosciences, Franklin Lakes, NJ, USA), as described in previous papers [11,14,15]. Briefly, 25–30  $\mu\text{g}$  of BDEV was subjected to Western blot under reducing (Hsp70, Flot-1, GM130) and non-reducing (CD81, CD63, Hsp90) conditions using 4–12% Bis-tris gels (Invitrogen, Waltham, MA, USA).

For YWHAH validation, 15  $\mu\text{g}$  of BDEV was subjected to Western blot under reducing conditions using 10% Bis-tris gel (Invitrogen, Waltham, MA, USA) against YWHAH (15222-1-AP, Proteintech, Rosemont, IL, USA). Primary and secondary antibody dilutions were carried out according to the manufacturer's suggestions. Blots were developed using Azure C Series Imager (Azure Biosystems, Dublin, CA, USA) with SuperSignal West Pico Chemiluminescent Substrate (Thermo Scientific, Waltham, MA, USA).

#### 2.5. TEM acquisition and Analysis

Transmission electron microscopy (TEM) on the BDEVs from saline and MDZ samples was performed as described in our previous studies [11,14,15]. Post-isolation, BDEV pellets were briefly suspended in 1X particle-free PBS. Then, 10  $\mu\text{L}$  of the BDEV suspension was combined with 90  $\mu\text{L}$  of the TEM fix buffer (2% glutaraldehyde, 2% paraformaldehyde, and 0.1 M phosphate buffer). Next, 10  $\mu\text{L}$  of the sample was added onto a mesh copper grid for 2 min and subsequently drawn up using a piece of filter paper. The left-over film was allowed to dry for 2 min. NanoVan negative stain was later added onto the grid, drawn up via filter paper, and allowed to dry before imaging on a Tecnai G2 Transmission Electron Microscope (FEI, Hillsboro, OR, USA) that operated at 80 kV.

#### 2.6. Zeta View Analysis

To comprehensively analyze the EVs' size distributions and particle concentration information, we utilized ZetaView nanoparticle tracking analyzer PMX120 (Particle Metrix, Inning am Ammersee, Germany) along with the software ZetaView 8.05.12 SP2 as previously described [16]. The instrument was calibrated using 100 nm polystyrene nano standard particles prior to the actual analysis. A total of 10  $\mu\text{L}$  of the sample was diluted to 1:10,000–1:30,000 in particle-free 1X PBS before loading to the instrument. Once samples were loaded, cell quality and particle drift were checked before capturing the video. The video was captured at a sensitivity of 65, a shuttle speed of 100, and a frame rate of 30 frames/s. The sample's size (in nm) and concentration (in particle/mL) were determined after being read at 11 positions for three cycles.

#### 2.7. RNA Extraction and RT-qPCR

Total RNA from the brain cortex was isolated from the randomly selected P21 pups ( $n = 12$ ) from each treatment group at P21 using the Direct-Zol RNA kit (Zymo Research, Irvine,

CA, USA) based on the manufacturer's protocol. The total amount of extracted RNA was quantified by Epoch2 (BioTek Instruments, Winooski, VT, USA). RNA was then converted to cDNA using the Superscript IV kit (Invitrogen, Waltham, MA, USA). The expressions of ESCRT complexes (ESCRT-0, -I, -II, and -III) were detected by qPCR using a pre-designed TaqMan™ Array 96-Well FAST Plate (REF#: 4413259, appliedbiosystems, Pleasanton, CA, USA) and QuantStudio™ 7 Flex Real-Time PCR System (cat: 4485701, appliedbiosystems, Pleasanton CA, USA). The TaqMan Plate consisted of 18S and GAPDH as housekeeping genes. Relative fold change was calculated based on the  $2^{-\Delta\Delta CT}$  method. The list of TaqMan probes and the overall plate design are included in Table S4.

### 2.8. Proteomics Analysis

Protein quantification was performed using Pierce BCA protein assay (Thermo Scientific, Rockford, IL, USA) and followed the procedure described in our earlier studies [3,17]. 50 µg of protein per sample from 6 animals was subjected to mass spectrometry (MS) analysis. MS analysis was established and managed with a UNMC Mass Spectrometry Core (Omaha, NE, USA). The analysis was based on the label-free quantitative mass spectrometry protocol. The details of the MS protocol and reagents used are described in our recently published studies [3,17].

The in-house mascot 2.6.2. (Matrix Science, Boston, MA, USA) search engine was used further to identify the proteins from tandem mass spectrometry data, as described in our published studies [3,17]. The search targeted total tryptic peptides and allowed for two missed cleavage sites. Carbamidomethylation of cysteine was set as a fixed modification. Acetylation of protein N-terminus and oxidized methionine were included as variable modifications. The highest permitted fragment mass error was 0.02 Da, and the precursor mass tolerance threshold was set at 10 ppm. A false discovery rate (FDR) of  $\leq 1\%$  was used to calculate the significance threshold of the ion score. Qualitative analysis was performed using proteogenomics QI proteomics 4.1 (Nonlinear Dynamics, Milford, MA, USA).

### 2.9. Bioinformatics Analysis

Proteins were established as differentially expressed utilizing criteria of a *t*-test *p*-value  $< 0.05$ , a minimum of 2 unique peptides, and an absolute fold-change  $\geq 1.5$ . Utilizing the Cytoscape plug-in ClueGO [18], gene ontology analysis was performed on the differentially expressed proteins (DEPs). Specifically, molecular functions and biological processes were targeted for GO enrichment analysis. A heatmap of all DEPs was created by employing function heatmap.2 in R (version 3.6.0) package, *gplots* [19].

### 2.10. Statistical Analysis

Post normalization, an unpaired *t*-test was conducted to detect significant DEPs following exposure to MDZ. Proteins with *p*-value  $< 0.05$ ,  $\geq 2$  unique peptides, and an absolute fold-change  $\geq 1.5$  were considered significant. The downregulation of YWHAH was established as significant, utilizing a student's unpaired *t*-test following Welch's correction with *p*  $< 0.05$ . All statistical analysis was conducted using GraphPad Prism version 9.4 (LA Jolla, CA, USA).

## 3. Results

### 3.1. Repetitive Exposure of MDZ during Early Development Influences BDEV Size in the Brain

To elucidate whether long-term MDZ exposure impacts BDEV composition and subsequent protein cargo, we isolated BDEV from both saline (control) and MDZ (experimental) groups utilizing the ultracentrifugation method from the multiple sucrose gradients, as described in our previous studies [11,14,15]. We then evaluated the purity of isolated BDEV by means of Western blot analysis against positive and negative EV markers, which were established by the International Society for Extracellular Vesicles [20]. Figure 1A shows the presence of the positive markers Hsp70, Hsp90, Flotillin-1, CD63, and CD81 in the BDEVs and the absence of EVs in the negative marker GM130. ZetaView analysis showed a

slight increase in the number of BDEVs released in post long-term MDZ exposure animals; however, the overall results were not significant (Figure 1B). All original blots containing all replicates are shown in Figure S1.

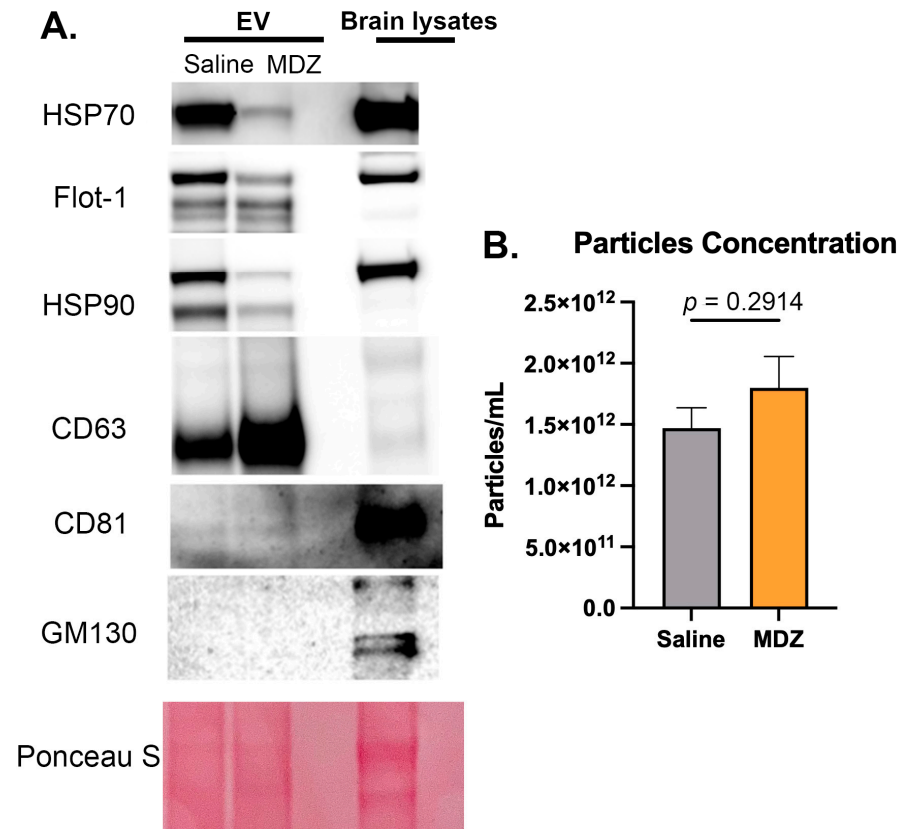


**Figure 1. Validation of BDEV purity.** (A) Western blot analysis on BDEV isolated from a control saline animal shows the expression of the positive markers Hsp70, Flot-1, Hsp90, CD63, and CD81. The negative marker GM130 was enriched in the whole brain lysate but absent in the EV fraction. Equal loading was confirmed via Ponceau S stain. (B) ZetaView nanoparticle tracking analysis shows a slight increase in BDEV particle concentration in rats exposed to MDZ ( $n = 18/\text{group}$ ). However, there were no significant changes in the concentrations of isolated BDEVs from the two groups as determined by an unpaired  $t$ -test following Welch's correction. Data are represented as Mean  $\pm$  SEM.

TEM analysis showed that BDEV particles had sphere-like shapes, and the most abundant size of the vesicles was around 200–300 nm in diameter (Figure 2). The BDEV size was not heavily influenced by long-term exposure to MDZ. Despite the insignificance of the results, smaller BDEV (<50 nm) was lesser abundant in the MDZ exposure ( $p = 0.063$ ).

### 3.2. Chronic MDZ Exposure during Early Development Does Not Impact BDEV Biogenesis

Based on the slight increase in particle concentration and relatively larger BDEV particles in the MDZ-exposed groups, we next evaluated if early long-term exposure to MDZ impacts EV biogenesis machinery. Accordingly, using RT-qPCR, we looked at the expression levels of key Endosomal Sorting Complex Required for Transport (ESCRT) genes, which regulate EV biogenesis. As seen in Figure 3, we did not observe any significant changes in the different genes associated with the ESCRT complexes, suggesting that long-term exposure to MDZ during early development does not impact BDEV biogenesis.

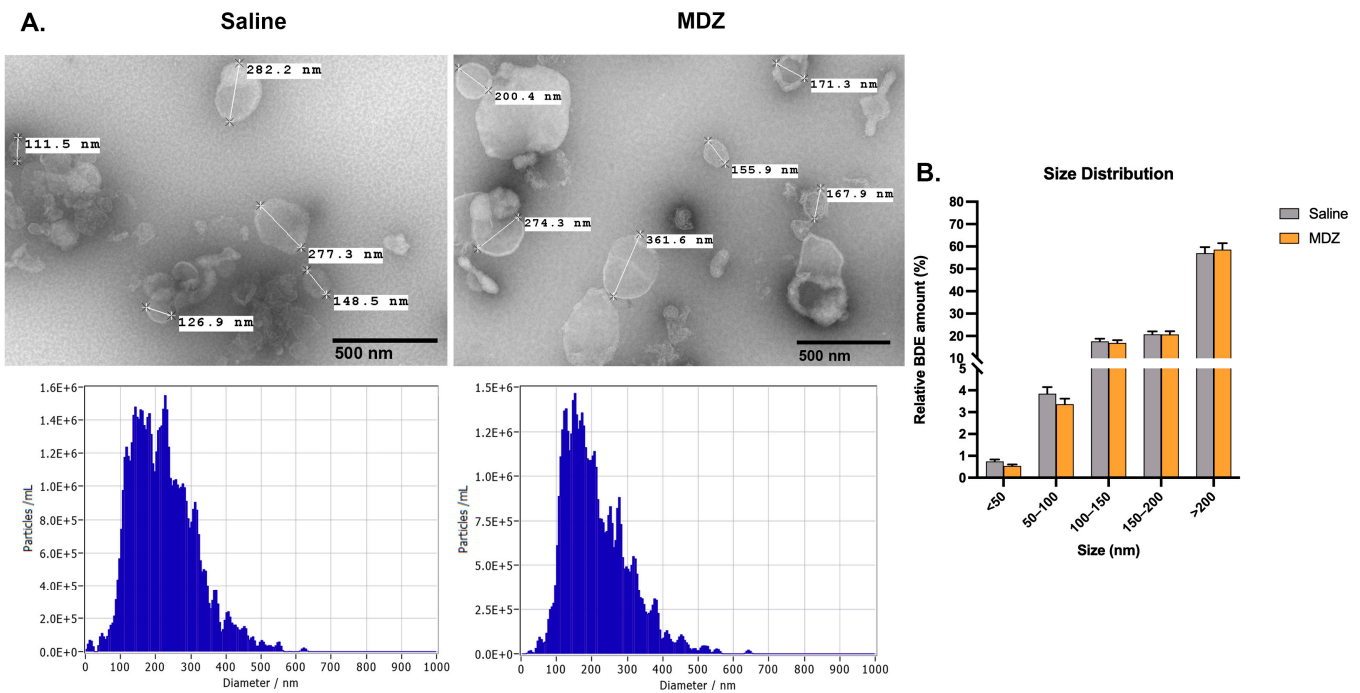


**Figure 2. Characterization of BDEV.** (A) BDEV isolated using a sucrose density gradient from the two groups was characterized using TEM (top), and Zeta-view analysis revealed no change in the sizes of particles with/without MDZ exposure (bottom). (B) Zeta-view analysis shows the different size distributions. Each group’s average BDEV sizes (in nm) are represented as Mean ± SEM (n = 18/group). Statistical significance is determined by multiple *t*-tests followed by Holm–Sidak correction.

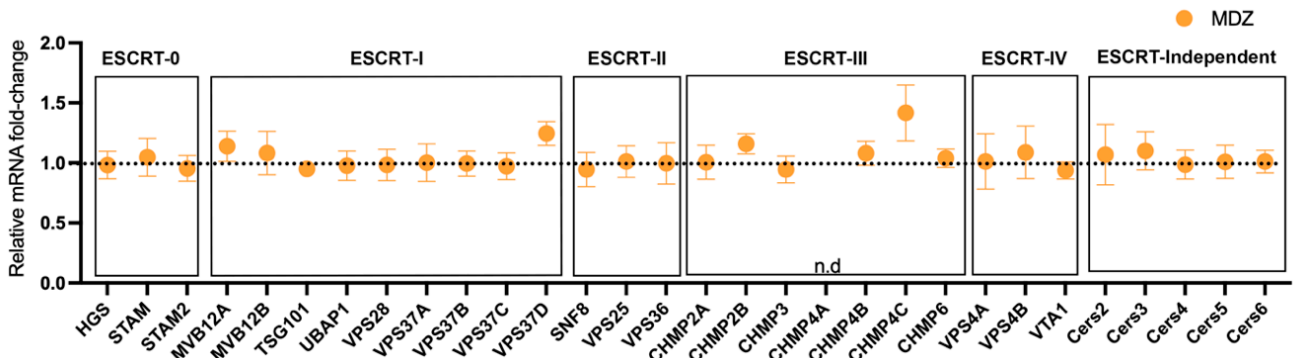


**Figure 3.** Long-term MDZ exposure during early development did not alter the biogenesis and the expression of ESCRT-dependent and independent pathway proteins. A custom qRT-PCR panel for EV biogenesis genes illustrated that genes involved in the ESCRT dependent (complexes 0, I, II, and III) and independent pathways did not alter upon exposure to MDZ (orange dot). Dotted line represents a baseline for Saline fold-change expression. Data represented as Mean ± SEM, n = 12/group, analyzed with a multiple *t*-test followed by Holm–Sidak correction. n.d. = no data, no amplification observed.

### 3.3. Long-Term MDZ Exposure Alters the Proteome in EV Cargo

Whilst no significant changes were observed in the BDEV biogenesis, we next tested whether long-term MDZ exposure during the early stages of life induced alterations in the BDEV proteome. Accordingly, we subjected P21-purified BDEV from the control and MDZ groups to high throughput quantitative mass-spectrometry-based proteomics. A total of 3328 proteins were identified (Table S1). Further employing a criterion of 2+ unique peptides, and *p* < 0.05, we identified 15 proteins to be differentially expressed between the two groups (Table 1). The heatmap (Figure 4) highlighted the differentially expressed

proteins (DEPs) after MDZ exposure based on a criterion of 1.5 absolute fold-change and  $p < 0.05$ . A total of eight proteins were up-regulated, while seven were down-regulated with respect to the control group.

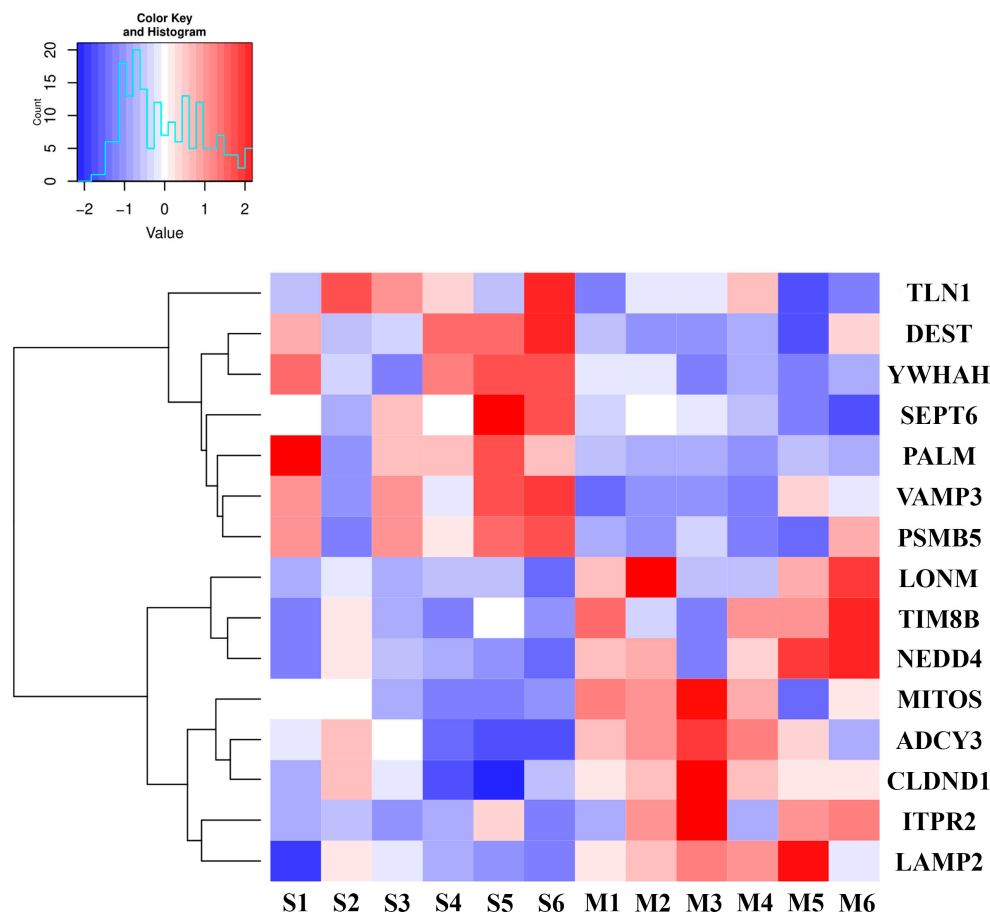


**Figure 4.** Differential expression of BDEV proteins in male and female rats post MDZ exposure. Heatmap showing the DEPs between the Midazolam and saline. S—Saline, M—Midazolam. Data were obtained from all six biological replicates from each group.

**Table 1.** Significant DEPs in P21 BDEVs after MDZ exposure. A criterion of 2+ unique peptides and an absolute fold change of >1.5 were used to select the potential hits. (+) and (−) sign represents up- and down-regulation, respectively, with respect to Saline samples.

Accession Number	Description (Protein Name)	Fold-Change
P62078	Mitochondrial import inner membrane translocase subunit (TIMM8B)	+3.86
Q9245D5	Lon protease homolog, mitochondrial (LONP1)	+2.99
Q5RKI8	Mitochondrial potassium channel ATP-binding subunit (ABCBC8)	+2.65
P21932	Adenylate cyclase type 3 (ADCY3)	+2.23
P29995	Inositol 1,4,5-trisphosphate receptor type 2 (ITPR2)	+2.07
Q62940	E3 ubiquitin-protein ligase (NEDD4)	+2.01
P17046	Lysosome-associated membrane glycoprotein 2 (LAMP2)	+1.91
G3B674	Claudin domain containing 1, isoform CRA_b (CLDND1)	+1.89
A0A0U1RRT8	Septin (SEPT6)	−2.24
P63025	Vesicle-associated membrane protein 3 (VAMP3)	−2.30
G3V852	RCG55135, isoform CRA_b (TLN1)	−2.32
Q7M0E3	Destrin (DSTN)	−2.58
G3V7Q6	Proteasome subunit beta (PSMB5)	−2.74
P68511	14-3-3 protein eta (YWHAH)	−3.27
Q920Q0	Paralemmin-1 (PALM)	−5.43

### 3.4. Gene Ontology Analysis of BDEV Reveals Potential Processes and Functions Associated with Long-Term MDZ Exposure

We next analyzed the biological processes and molecular functions enriched with these DEPs (Figures 5 and 6) using the bioinformatics tool ClueGO analysis. The most abundant biological process was the corticosteroid receptor signaling pathway, with 30.0% of gene ontology (GO) terms associated with this process, followed by olfactory learning, regulation of adenylate activity, integrin activation, and the rest of the processes reported in Figure 5A, which all shared 10% of the GO terms. For the molecular function, 28.57% of DEPs are associated with the sodium channel activity and adenylate cyclase activity, while other molecular functions include ATP-dependent peptidase activity, LIM domain binding, and Inositol 1,4,5 trisphosphate binding, which all account equally for 14.29% of GO terms (Figure 6A). Figures 5B and 6B represent all the possible connections and networks of those DEPs associated with GO terms and groups of functions or processes. A complete list of GO terms and associated genes can be found in Table S2 (biological processes) and Table S3 (molecular functions).

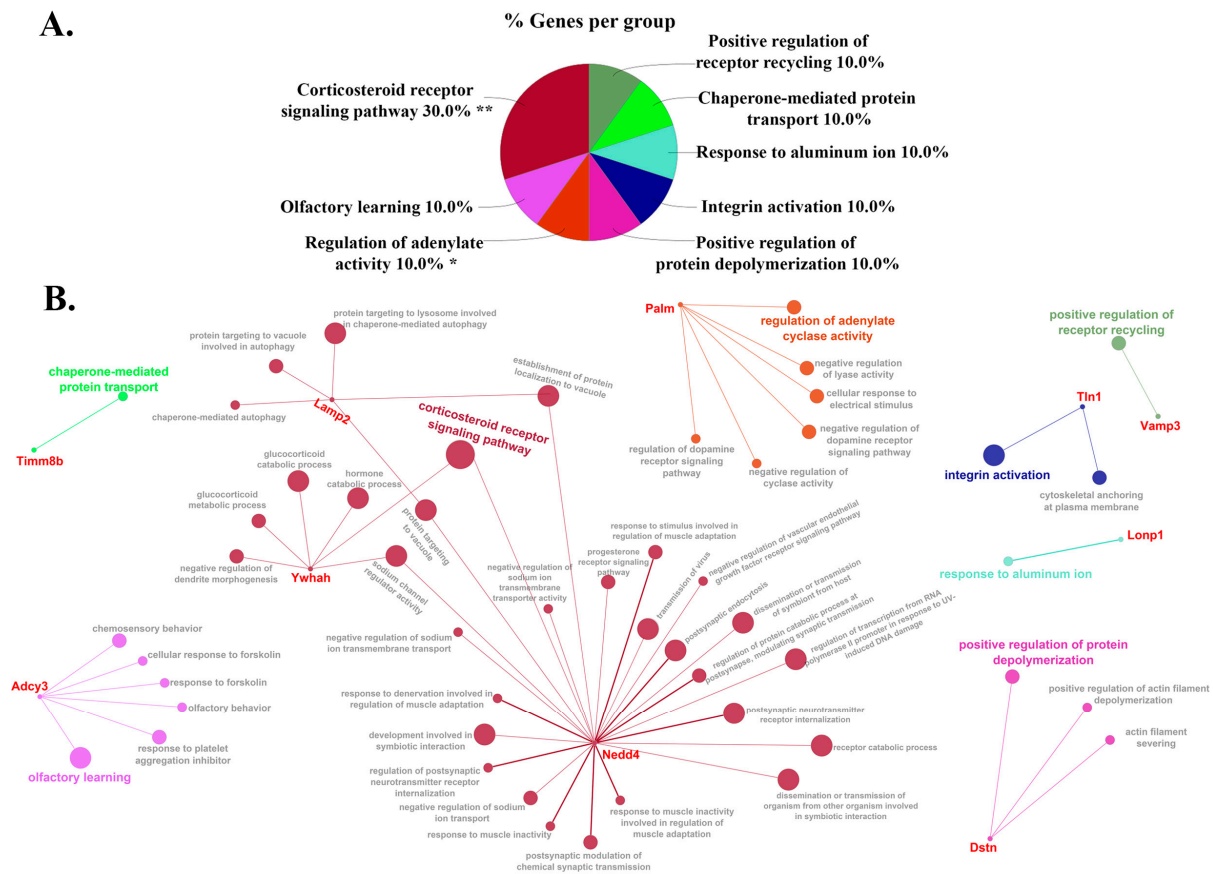


**Figure 5.** (A) Percentage of genes per group mapped to biological processes and (B) networks shows the interaction of proteins and their biological process for the DEPs using ClueGO. The asterisks represent the group term *p*-value representing each category. \* *p* < 0.05 and \*\* *p* < 0.01.

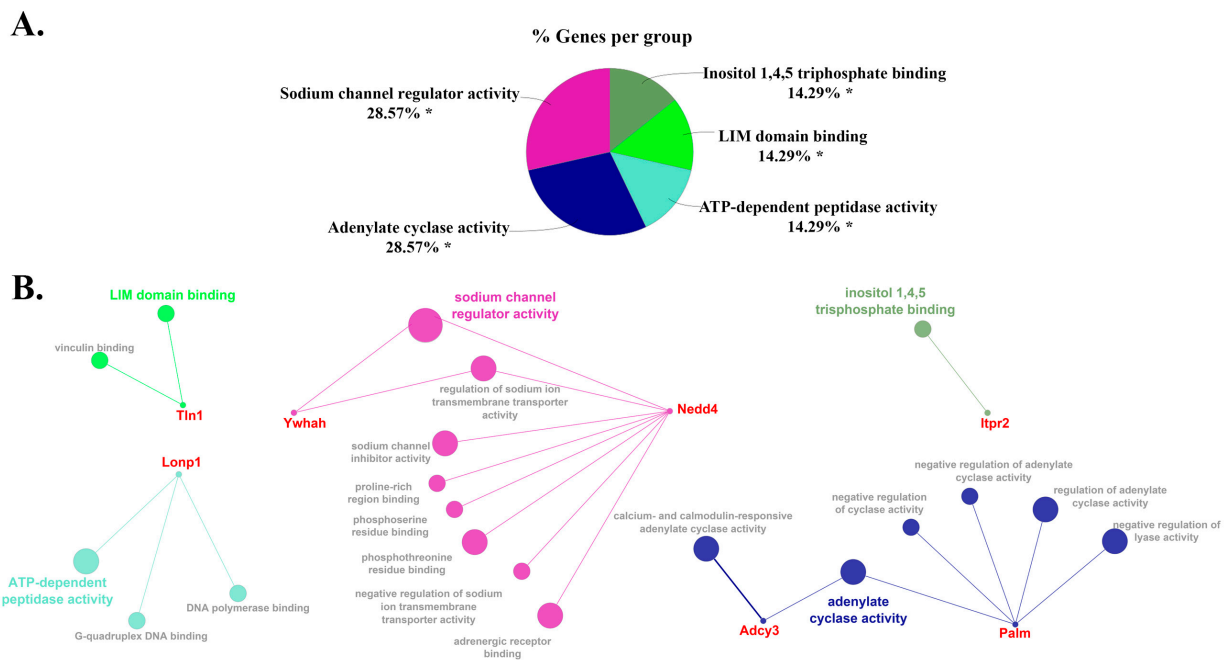


**Figure 6.** (A) Percentage of genes per group mapped to molecular functions and (B) networks shows the interaction of proteins and their molecular function for the DEPs using ClueGO. The asterisks represent the group term *p*-value representing each category. \* *p* < 0.05.

### 3.5. Identification of YWHAH as a Novel BDEV Marker with Long-Term MDZ Exposure during Early Development

The high-throughput proteomics generated several possible hits, and further validation was necessary. One hit we successfully identified and validated was 14-3-3 eta protein (YWHAH), an adapter protein responsible for intracellular signaling and regulatory pathways. YWHAH was down-regulated −3.27-fold in the MDZ-treated group (Table 1), and its protein expression change was further validated with Western Blot (Figure 7). All original blots containing all replicates are shown in Figure S2.

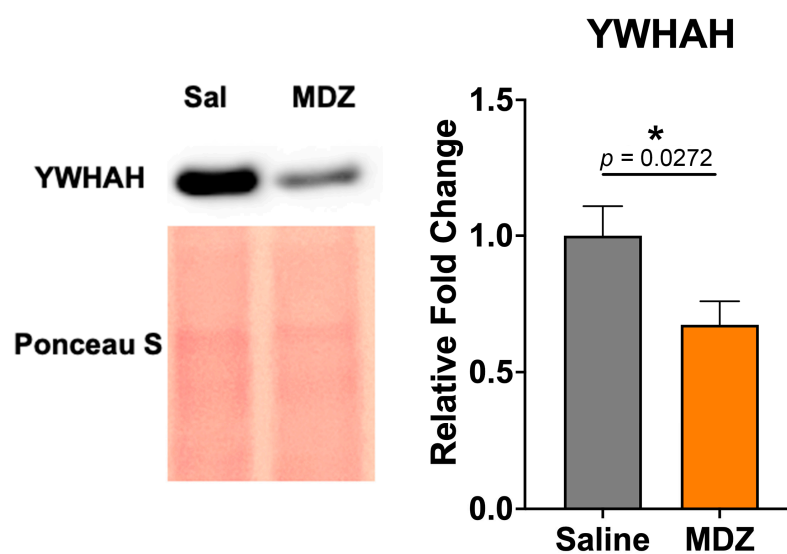


**Figure 7. Validation of YWHAH after MDZ exposure.** A representative Western Blot is depicted. Data is represented as Mean ± SEM (n = 13/group), and significance was determined with an unpaired *t*-test after Welch’s correction. \* *p* = 0.0272.

#### 4. Discussion

The current study for the first time aims to decode how chronic long-term exposure to the sedative benzodiazepine MDZ during the early stages of development impacts the overall BDEV function. The main findings from our study underlined the up- and down-regulated differentially expressed proteins (DEPs) in the BDEV cargo that are potentially involved in various molecular functions (e.g., sodium channel regulatory, adenylate cyclase, and ATP-dependent peptidase activities) and biological processes (e.g., corticosteroid receptor signaling pathway, regulation of adenylate activity, and positive regulation of protein depolymerization). The results from our study provide new aspects concerning long-term MDZ exposure during early development, potentially affecting intercellular neural signaling and overall molecular functions.

In our study, we did not observe a significant difference in the size distribution of EVs, which implied that there is no difference in the EV subpopulations in the brain post MDZ exposure. However, we observed an interesting trend regarding the number of EVs released between saline and MDZ-exposed brains. Specifically, the total amount of particles produced by the MDZ group is slightly higher and more abundant at a larger size than the control (Figures 1B and 2B). This suggests alterations in the inner EV cargo materials that affect EV size. Since we observed a heterogenous subpopulation of EVs in the brain, we further characterized the DEPs on the EV cargo.

In the developing brain, regular EV release contributes to normal brain development since EVs play an essential role in cell-to-cell communication in the central nervous system (CNS) [21]. The CNS structure, function, and homeostasis depend on cell-to-cell communication throughout the lifespan [22]. Notably, materials such as proteins, microRNA, lipids, etc., packed in the EV cargo could be characterized into biomarkers. Neurogenesis, gliogenesis, synaptogenesis, and myelination, are major CNS processes that start at the beginning of life and are critical for assuring the proper development in the brain to proceed to adulthood [23]. Therefore, any internal or external insults to the brain, such as exposure to neurotoxicity substances, during these critical processes will alter the brain's homeostasis and make it more vulnerable to normal development. Studies established by Fauré et al. and Lachenal et al. implied that EVs could act as disposal mechanisms in synapses, where lysosomes are absent, to discard synaptic receptors as a response to the alterations of synaptic plasticity [24,25]. Notably, in many preclinical and clinical studies, exposure to MDZ during early developmental periods has been associated with alteration of synaptic plasticity subsequently leading to impaired cognitive function and an increased risk of developing learning disorders [26–29].

Interestingly, this study identified a connection between DEPs and potential networks associated with synaptic and disposable functions in the cell. Our network analysis based on ClueGO biological processes showed the association between E3 ubiquitin-protein ligase (NEDD4) and lysosome-associated membrane glycoprotein (LAMP2) proteins in targeting the vacuole (Figure 5), which is an organelle that helps sequester waste product in animal cells [30]. NEDD4 and LAMP2 are up-regulated in our Midazolam-exposed BDEVs (Figure 3 and Table 1). Importantly, in the CNS, up-regulation of NEDD4 has been noted in several neurodegenerative diseases such as Alzheimer's, Parkinson's disease, and Huntington's disease [31,32]. Furthermore, Kwak et al.'s 2012 study pointed out that the increase in transcriptional activation of NEDD4 results from the escalation in neurotoxins and oxidative stress present in the brain [31]. On the other hand, the functional role of LAMP2 is maintaining lysosomal stability and actively participating in autophagy [33]. In neuropathology, LAMP2 concentration has been reported to be decreased in the patient's cerebrospinal fluid (CSF) of Parkinson's disease [34,35] and increased in patients with Alzheimer's [36,37]. Further research would need to invest in determining the mechanism of why these proteins are packed more into the EV cargo, whether it would be a protection mechanism of the brain to cope with the repetitive exposure to MDZ, or if it would be a sort of biomarker that acts as an early onset signal for a developing neuropathology.

Our ClueGO analysis (Figures 5 and 6) also revealed that the molecular and biological processes are mainly associated with sodium channel activity. One of the proteins related to this group that we identified was protein 14-3-3 eta or YWHAH. The 14-3-3 proteins, also known as YWHAx, where the “x” is a representation for isoforms including  $\beta$ ,  $\gamma$ ,  $\epsilon$ ,  $\zeta$ ,  $\eta$ ,  $\theta$ , and  $\sigma$  that are encoded by seven genes (*YWHAH/G/E/Z/H/Q/S*, respectively), is a highly conserved protein. YWHAx proteins are involved in many crucial cellular processes such as metabolism, protein trafficking, signal transduction, apoptosis, cell cycle regulation, transcription, stress responses, and malignant transformation [38]. With 14-3-3 proteins having a wide range of cellular and molecular roles and functions, it's no surprise that this family is linked to various human disorders [39]. Some human diseases associated with 14-3-3 protein dysfunction are cardiomyopathy, cancer, and even hair pigmentation [39]. Notably, the YWHAx family is highly conserved and abundant in the brain, accounting for 1% soluble protein [40]. Since YWHAx proteins are the most abundant in the brain and are frequently present in cerebrospinal fluid in neurodegenerative illnesses, they may play a crucial role in the physiology and death of neurons [41]. In recent decades, the importance of the YWHAx family has been highlighted in various neurological and neuropsychiatric disorders, including schizophrenia, bipolar disorders, Parkinson's disease, Alzheimer's disease, and Creutzfeldt–Jakob disease [41,42].

Intriguingly, over the past decade, evidence has emerged that the 14-3-3 family is essential for the development of the nervous system, and especially cortical development. More recently, the 14-3-3 family has been recognized as a crucial regulator in several neurodevelopmental processes. Our results revealed that YWHAH was significantly down-regulated in proteomics data and Western blot (Figures 4 and 7). A study by Kwon et al. demonstrated that ischemia injury decreased YWHAH expression in the hippocampus sub-regions. Moreover, the expression of YWHAH was also found to be decreased in kainic acid-induced neurotoxicity [43]. Another study conducted by Buret et al. pointed out that mice with YWHAH deficiency led to the impairment of outer and inner hair cells, and variants of YWHAH would lead to mitochondria fragmentation, making the cells more susceptible to apoptosis [41]. Noteworthy, these studies established the idea that the downregulation, imbalance, or dysfunction of YWHAH could be highly associated with subsequent neuronal loss, which eventually contributes to the development of neurodegenerative diseases. Evidence shows that more neuronal cell death occurs when exposed to MDZ in many *in vitro* and *in vivo* studies [5,28,44]. Thus, the downregulation of YWHAH post-MDZ exposure could possibly be implicated in neuronal cell death.

## 5. Conclusions

Our study for the first time performed a comprehensive analysis on how long term MDZ exposure at early development can brain function. Notably, using state of the art high throughput technologies, we mined the BDEV proteome and identified including validating the expression of YWHAH as a potential target. Future studies are aimed at further characterization of its downstream mechanisms both *in vitro* and *in vivo* and thus could pave way to develop it as a potential therapeutic to mitigate altered brain development with long term MDZ exposure in neonates.

**Supplementary Materials:** The following supporting information can be downloaded at: <https://www.mdpi.com/article/10.3390/cells12060966/s1>, Figure S1: Validation of BDEV markers. Individual western blots on isolated BDEVs were used in the study. Ponceau-stained membranes are at the bottom for each membrane. Boxed blots are shown in Figure 1 of the manuscript. S-Saline, MDZ-Midazolam, BL-Brain Lysate. Figure S2: Individual western blots on isolated BDEVs in all 13 BDEV samples/groups used in the study. Boxed blots are shown in Figure 7 of the manuscript. S-Saline, MZ-Midazolam. Table S1: Proteomics hits on brain-derived extracellular vesicles. Table S2: Biological Processes GO terms associated with DEPs. Table S3: Molecular Function GO terms associated with DEPs. Table S4: Multiplex RNA information.

**Author Contributions:** Conceptualization: N.M.N., S.V.Y. and G.P.; investigation: N.M.N., D.M., L.M., S.C. and M.M.; formal analysis: N.M.N., S.J. and C.G.; data curation: S.J. and C.G.; writing—original draft: N.M.N. and D.M.; visualization: N.M.N., S.J. and C.G.; writing—review and editing: S.C., S.J., S.V.Y. and G.P.; supervision: S.V.Y. and G.P.; project administration: G.P.; funding acquisition: S.V.Y. and G.P. All authors have read and agreed to the published version of the manuscript.

**Funding:** This research was funded by Start-up funds from the Department of Anesthesiology (S.V.Y. and G.P.), the Lieberman Research Endowment and R21DA049577 to G.P.

**Institutional Review Board Statement:** The study was conducted in accordance with the National Institutes of Health Guide for the Care and Use of Laboratory Animals and approved by the Institutional Animal Care and Use Committee (IACUC) of the University of Nebraska Medical Center (protocol: 19-130).

**Informed Consent Statement:** Not applicable.

**Data Availability Statement:** Data are contained within the article and additional data in the Supplementary Files.

**Acknowledgments:** We would like to thank the Mass Spectrometry Proteomics Core Facility and Electron Microscopy core Facility at UNMC for their assistance with mass spectrometry analysis and TEM data acquisition.

**Conflicts of Interest:** The authors declare no conflict of interest.

## References

- Duerden, E.G.; Guo, T.; Dodbibba, L.; Chakravarty, M.M.; Chau, V.; Poskitt, K.J.; Synnes, A.; Grunau, R.E.; Miller, S.P. Midazolam dose correlates with abnormal hippocampal growth and neurodevelopmental outcome in preterm infants. *Ann. Neurol.* **2016**, *79*, 548–559. [[CrossRef](#)]
- Durrmeyer, X.; Vutskits, L.; Anand, K.J.S.; Rimensberger, P.C. Use of Analgesic and Sedative Drugs in the NICU: Integrating Clinical Trials and Laboratory Data. *Pediatr. Res.* **2010**, *67*, 117–127. [[CrossRef](#)] [[PubMed](#)]
- Nguyen, N.M.; Vellichirammal, N.N.; Guda, C.; Pendyala, G. Decoding the Synaptic Proteome with Long-Term Exposure to Midazolam during Early Development. *Int. J. Mol. Sci.* **2022**, *23*, 4137. [[CrossRef](#)] [[PubMed](#)]
- McPherson, C. Sedation and analgesia in mechanically ventilated preterm neonates: Continue standard of care or experiment? *J. Pediatr. Pharmacol. Ther.* **2012**, *17*, 351–364. [[CrossRef](#)] [[PubMed](#)]
- Young, C.; Jevtovic-Todorovic, V.; Qin, Y.Q.; Tenkova, T.; Wang, H.; Labruyere, J.; Olney, J.W. Potential of ketamine and midazolam, individually or in combination, to induce apoptotic neurodegeneration in the infant mouse brain. *Br. J. Pharmacol.* **2005**, *146*, 189–197. [[CrossRef](#)]
- Lin, H.; Chen, H.; Qi, B.; Jiang, Y.; Lian, N.; Zhuang, X.; Yu, Y. Brain-derived extracellular vesicles mediated coagulopathy, inflammation and apoptosis after sepsis. *Thromb. Res.* **2021**, *207*, 85–95. [[CrossRef](#)]
- György, B.; Szabó, T.G.; Pásztói, M.; Pál, Z.; Misják, P.; Aradi, B.; László, V.; Pállinger, E.; Pap, E.; Kittel, A.; et al. Membrane vesicles, current state-of-the-art: Emerging role of extracellular vesicles. *Cell. Mol. Life Sci.* **2011**, *68*, 2667–2688. [[CrossRef](#)]
- Théry, C.; Ostrowski, M.; Segura, E. Membrane vesicles as conveyors of immune responses. *Nat. Rev. Immunol.* **2009**, *9*, 581–593. [[CrossRef](#)]
- Antonyak, M.A.; Li, B.; Boroughs, L.K.; Johnson, J.L.; Druso, J.E.; Bryant, K.L.; Holowka, D.A.; Cerione, R.A. Cancer cell-derived microvesicles induce transformation by transferring tissue transglutaminase and fibronectin to recipient cells. *Proc. Natl. Acad. Sci. USA* **2011**, *108*, 4852–4857. [[CrossRef](#)]
- Holmgren, L.; Szeles, A.; Rajnavölgyi, E.; Folkman, J.; Klein, G.; Ernberg, I.; Falk, K.I. Horizontal transfer of DNA by the uptake of apoptotic bodies. *Blood* **1999**, *93*, 3956–3963. [[CrossRef](#)]
- Koul, S.; Schaal, V.L.; Chand, S.; Pittenger, S.T.; Nantho Vellichirammal, N.; Kumar, V.; Guda, C.; Bevens, R.A.; Yelamanchili, S.V.; Pendyala, G. Role of Brain Derived Extracellular Vesicles in Decoding Sex Differences Associated with Nicotine Self-Administration. *Cells* **2020**, *9*, 1883. [[CrossRef](#)] [[PubMed](#)]
- Raposo, G.; Stoorvogel, W. Extracellular vesicles: Exosomes, microvesicles, and friends. *J. Cell Biol.* **2013**, *200*, 373–383. [[CrossRef](#)] [[PubMed](#)]
- Maas, S.L.N.; Breakefield, X.O.; Weaver, A.M. Extracellular Vesicles: Unique Intercellular Delivery Vehicles. *Trends Cell Biol.* **2017**, *27*, 172–188. [[CrossRef](#)] [[PubMed](#)]
- Chand, S.; Gowen, A.; Savine, M.; Moore, D.; Clark, A.; Huynh, W.; Wu, N.; Odegaard, K.; Weyrich, L.; Bevens, R.A.; et al. A comprehensive study to delineate the role of an extracellular vesicle-associated microRNA-29a in chronic methamphetamine use disorder. *J. Extracell. Vesicles* **2021**, *10*, e12177. [[CrossRef](#)] [[PubMed](#)]
- Shahjin, F.; Guda, R.S.; Schaal, V.L.; Odegaard, K.; Clark, A.; Gowen, A.; Xiao, P.; Lisco, S.J.; Pendyala, G.; Yelamanchili, S.V. Brain-Derived Extracellular Vesicle microRNA Signatures Associated with In Utero and Postnatal Oxycodone Exposure. *Cells* **2019**, *9*, 21. [[CrossRef](#)] [[PubMed](#)]

16. Kannan, M.; Singh, S.; Chemparathy, D.T.; Oladapo, A.A.; Gawande, D.Y.; Dravid, S.M.; Buch, S.; Sil, S. HIV-1 Tat induced microglial EVs leads to neuronal synaptodendritic injury: Microglia-neuron cross-talk in NeuroHIV. *Extracell. Vesicles Circ. Nucleic Acids* **2022**, *3*, 133–149. [[CrossRef](#)]
17. Meyer, D.; Athota, P.; Gowen, A.; Nguyen, N.M.; Schaal, V.L.; Yelamanchili, S.V.; Pendyala, G. Effect of Combined Methamphetamine and Oxycodone Use on the Synaptic Proteome in an *In Vitro* Model of Polysubstance Use. *Genes* **2022**, *13*, 1816. [[CrossRef](#)]
18. Bindea, G.; Mlecnik, B.; Hackl, H.; Charoentong, P.; Tosolini, M.; Kirilovsky, A.; Fridman, W.H.; Pagès, F.; Trajanoski, Z.; Galon, J. ClueGO: A Cytoscape plug-in to decipher functionally grouped gene ontology and pathway annotation networks. *Bioinformatics* **2009**, *25*, 1091–1093. [[CrossRef](#)]
19. Warnes, G.R.; Bolker, B.; Bonebakker, L.; Gentleman, R.; Huber, W.; Liaw, A.; Lumley, T.; Maechler, M.; Magnusson, A.; Moeller, S. gplots: Various R programming tools for plotting data. *R. Package Version* **2009**, *2*, 1.
20. Théry, C.; Witwer, K.W.; Aikawa, E.; Alcaraz, M.J.; Anderson, J.D.; Andriantsitohaina, R.; Antoniou, A.; Arab, T.; Archer, F.; Atkin-Smith, G.K.; et al. Minimal information for studies of extracellular vesicles 2018 (MISEV2018): A position statement of the International Society for Extracellular Vesicles and update of the MISEV2014 guidelines. *J. Extracell. Vesicles* **2018**, *7*, 1535750. [[CrossRef](#)]
21. Schnatz, A.; Müller, C.; Brahmer, A.; Krämer-Albers, E.M. Extracellular Vesicles in neural cell interaction and CNS homeostasis. *FASEB Bioadv.* **2021**, *3*, 577–592. [[CrossRef](#)] [[PubMed](#)]
22. Bahram Sangani, N.; Gomes, A.R.; Curfs, L.M.G.; Reutelingsperger, C.P. The role of Extracellular Vesicles during CNS development. *Prog. Neurobiol.* **2021**, *205*, 102124. [[CrossRef](#)] [[PubMed](#)]
23. Semple, B.D.; Blomgren, K.; Gimlin, K.; Ferriero, D.M.; Noble-Haeusslein, L.J. Brain development in rodents and humans: Identifying benchmarks of maturation and vulnerability to injury across species. *Prog. Neurobiol.* **2013**, *106–107*, 1–16. [[CrossRef](#)] [[PubMed](#)]
24. Fauré, J.; Lachenal, G.; Court, M.; Hirrlinger, J.; Chatellard-Causse, C.; Blot, B.; Grange, J.; Schoehn, G.; Goldberg, Y.; Boyer, V.; et al. Exosomes are released by cultured cortical neurones. *Mol. Cell. Neurosci.* **2006**, *31*, 642–648. [[CrossRef](#)]
25. Lachenal, G.; Pernet-Gallay, K.; Chivet, M.; Hemming, F.J.; Belly, A.; Bodon, G.; Blot, B.; Haase, G.; Goldberg, Y.; Sadoul, R. Release of exosomes from differentiated neurons and its regulation by synaptic glutamatergic activity. *Mol. Cell. Neurosci.* **2011**, *46*, 409–418. [[CrossRef](#)]
26. Jevtovic-Todorovic, V.; Hartman, R.E.; Izumi, Y.; Benshoff, N.D.; Dikranian, K.; Zorumski, C.F.; Olney, J.W.; Wozniak, D.F. Early exposure to common anesthetic agents causes widespread neurodegeneration in the developing rat brain and persistent learning deficits. *J. Neurosci.* **2003**, *23*, 876–882. [[CrossRef](#)]
27. Iqbal O'Meara, A.M.; Miller Ferguson, N.; Zven, S.E.; Karam, O.L.; Meyer, L.C.; Bigbee, J.W.; Sato-Bigbee, C. Potential Neurodevelopmental Effects of Pediatric Intensive Care Sedation and Analgesia: Repetitive Benzodiazepine and Opioid Exposure Alters Expression of Glial and Synaptic Proteins in Juvenile Rats. *Crit. Care Explor.* **2020**, *2*, e0105. [[CrossRef](#)]
28. Xu, J.; Mathena, R.P.; Singh, S.; Kim, J.; Long, J.J.; Li, Q.; Junn, S.; Blaize, E.; Mintz, C.D. Early Developmental Exposure to Repetitive Long Duration of Midazolam Sedation Causes Behavioral and Synaptic Alterations in a Rodent Model of Neurodevelopment. *J. Neurosurg. Anesthesiol.* **2019**, *31*, 151–162. [[CrossRef](#)]
29. Tokuda, K.; O'Dell, K.A.; Izumi, Y.; Zorumski, C.F. Midazolam inhibits hippocampal long-term potentiation and learning through dual central and peripheral benzodiazepine receptor activation and neurosteroidogenesis. *J. Neurosci.* **2010**, *30*, 16788–16795. [[CrossRef](#)]
30. Wada, Y. Vacuoles in mammals: A subcellular structure indispensable for early embryogenesis. *Bioarchitecture* **2013**, *3*, 13–19. [[CrossRef](#)]
31. Kwak, Y.D.; Wang, B.; Li, J.J.; Wang, R.; Deng, Q.; Diao, S.; Chen, Y.; Xu, R.; Masliah, E.; Xu, H.; et al. Upregulation of the E3 ligase NEDD4-1 by oxidative stress degrades IGF-1 receptor protein in neurodegeneration. *J. Neurosci.* **2012**, *32*, 10971–10981. [[CrossRef](#)]
32. Potjewyd, F.M.; Axtman, A.D. Exploration of Aberrant E3 Ligases Implicated in Alzheimer's Disease and Development of Chemical Tools to Modulate Their Function. *Front. Cell. Neurosci.* **2021**, *15*, 768655. [[CrossRef](#)]
33. Eskelinen, E.L.; Illert, A.L.; Tanaka, Y.; Schwarzmann, G.; Blanz, J.; Von Figura, K.; Saftig, P. Role of LAMP-2 in lysosome biogenesis and autophagy. *Mol. Biol. Cell* **2002**, *13*, 3355–3368. [[CrossRef](#)] [[PubMed](#)]
34. Boman, A.; Svensson, S.; Boxer, A.; Rojas, J.C.; Seeley, W.W.; Karydas, A.; Miller, B.; Kågedal, K.; Svenningsson, P. Distinct Lysosomal Network Protein Profiles in Parkinsonian Syndrome Cerebrospinal Fluid. *J. Park. Dis.* **2016**, *6*, 307–315. [[CrossRef](#)] [[PubMed](#)]
35. Klaver, A.C.; Coffey, M.P.; Aasly, J.O.; Loeffler, D.A. CSF lamp2 concentrations are decreased in female Parkinson's disease patients with LRRK2 mutations. *Brain Res.* **2018**, *1683*, 12–16. [[CrossRef](#)]
36. Armstrong, A.; Mattsson, N.; Appelqvist, H.; Janefjord, C.; Sandin, L.; Agholme, L.; Olsson, B.; Svensson, S.; Blennow, K.; Zetterberg, H.; et al. Lysosomal network proteins as potential novel CSF biomarkers for Alzheimer's disease. *Neuromol. Med.* **2014**, *16*, 150–160. [[CrossRef](#)]
37. Sjödin, S.; Öhrfelt, A.; Brinkmalm, G.; Zetterberg, H.; Blennow, K.; Brinkmalm, A. Targeting LAMP2 in human cerebrospinal fluid with a combination of immunopurification and high resolution parallel reaction monitoring mass spectrometry. *Clin. Proteom.* **2016**, *13*, 4. [[CrossRef](#)]
38. Darling, D.L.; Yingling, J.; Wynshaw-Boris, A. Role of 14-3-3 proteins in eukaryotic signaling and development. *Curr. Top. Dev. Biol.* **2005**, *68*, 281–315. [[CrossRef](#)] [[PubMed](#)]
39. Cornell, B.; Toyo-Oka, K. 14-3-3 Proteins in Brain Development: Neurogenesis, Neuronal Migration and Neuromorphogenesis. *Front. Mol. Neurosci.* **2017**, *10*, 318. [[CrossRef](#)] [[PubMed](#)]

40. Berg, D.; Holzmann, C.; Riess, O. 14-3-3 proteins in the nervous system. *Nat. Rev. Neurosci.* **2003**, *4*, 752–762. [[CrossRef](#)]
41. Buret, L.; Rebillard, G.; Brun, E.; Angebault, C.; Pequignot, M.; Lenoir, M.; Do-Cruzeiro, M.; Tournier, E.; Cornille, K.; Saleur, A.; et al. Loss of function of Ywhah in mice induces deafness and cochlear outer hair cells' degeneration. *Cell Death Discov.* **2016**, *2*, 16017. [[CrossRef](#)] [[PubMed](#)]
42. Foote, M.; Zhou, Y. 14-3-3 proteins in neurological disorders. *Int. J. Biochem. Mol. Biol.* **2012**, *3*, 152–164. [[PubMed](#)]
43. Smani, D.; Sarkar, S.; Raymick, J.; Kanungo, J.; Paule, M.G.; Gu, Q. Downregulation of 14-3-3 Proteins in a Kainic Acid-Induced Neurotoxicity Model. *Mol. Neurobiol.* **2018**, *55*, 122–129. [[CrossRef](#)] [[PubMed](#)]
44. Stevens, M.F.; Werdehausen, R.; Gaza, N.; Hermanns, H.; Kremer, D.; Bauer, I.; Küry, P.; Hollmann, M.W.; Braun, S. Midazolam activates the intrinsic pathway of apoptosis independent of benzodiazepine and death receptor signaling. *Reg. Anesth. Pain. Med.* **2011**, *36*, 343–349. [[CrossRef](#)] [[PubMed](#)]

**Disclaimer/Publisher's Note:** The statements, opinions and data contained in all publications are solely those of the individual author(s) and contributor(s) and not of MDPI and/or the editor(s). MDPI and/or the editor(s) disclaim responsibility for any injury to people or property resulting from any ideas, methods, instructions or products referred to in the content.